Proceedings of the ASME 2010 Dynamic Systems and Control Conference
DSCC2010
September 12-15, 2010, Cambridge, Massachusetts, USA

DSCC2010-4182

OBSERVER BASED TRANSIENT FUEL UTILIZATION CONTROL FOR SOLID OXIDE FUEL CELLS

Tuhin Das*
Department of Mechanical Engineering
Rochester Institute of Technology
Rochester, NY 14623
Email: tkdeme@rit.edu

Andrew Slippey
Department of Mechanical Engineering
Rochester Institute of Technology
Rochester, NY 14623

ABSTRACT

Transient control is important for prolonging the life of SOFCs and broadening their applications. This paper develops an observer based method for transient control. The essential idea is to regulate the fuel cell current using the estimated state, incorporated within a steady-state invariant property of the SOFC. The objective is to directly address hydrogen starvation in SOFCs through control of transient fuel utilization. The method is demonstrated for two different SOFC systems. The applicability across configurations indicates the possible validity of this approach for SOFCs in general. The control design is supported by simulation results.

INTRODUCTION

Among different fuel cell technologies, the Solid Oxide Fuel Cell (SOFC) technology has attracted significant interest in recent years due to high efficiency, internal reforming capability, fuel flexibility, tolerance to impurities and combined heat and power applications [1]. In spite of these favorable attributes, application of SOFCs has been limited due to their poor load following capability [2]. This is a common drawback of fuel cells that is magnified under aggressive power fluctuations. It is attributed to the slow dynamic response of the fuel and air delivery systems consisting of valves, pumps and reformers, [3, 4]. It is manifested as hydrogen or oxygen starvation and drastic voltage drop. In Polymer Electrolyte Membrane (PEM) fuel cells oxygen starvation is the main concern, whereas in SOFCs hydrogen starvation is the main issue.

For SOFCs, the dynamic limitations of the fuel cell are reflected in the transient response of a single performance variable, namely fuel utilization. Fuel utilization, U, is defined as the ratio of hydrogen consumption to the net available hydrogen in the anode of an SOFC. While high utilization implies high efficiency, very high utilization leads to reduced partial pressure of hydrogen in the anode, leading to voltage drop [4]. Typically, $80-90\%$ is set as the target range, [5, 6], for optimal efficiency. U must be maintained around an optimal value (say 85%) within narrow limits ($\pm 5\%$) even under significant power fluctuations, to ensure optimal performance while preventing hydrogen starvation.

Thus transient control of SOFCs is important. However, there is limited work in the literature that addresses this topic. In [7], a model predictive approach is used and in [8], starvation is addressed by using a linear compensator to modify the target fuel flow. For PEM fuel cells, where oxygen starvation is a greater issue, existing methods of mitigation include use of reference governors [9, 10], or Model Predictive Control (MPC) [3,11]. Although hydrogen starvation in SOFCs and oxygen starvation in PEMs have some similar effects such as excessive voltage drop, the two fuel cells are sufficiently different to warrant different approaches for addressing these phenomena. Most importantly, the fuel supply to SOFC anode is a gas mixture containing several species with varying and unknown concentrations due to fuel flexibility and internal reforming reactions. In contrast, in PEMs the air supply has a fixed and known amount of oxygen.

In this paper, we present a new, observer based approach to transient control of U that builds on our prior research [12]. The use of observers is motivated by our earlier work on observer designs for SOFC systems for estimating species concentrations [13]. In our prior research we have used a steady-state invariant property of SOFCs for transient control. This approach reduces computational complexity and leads to a simple control

*Address all correspondence to this author.

strategy. In this paper, we retain this simplicity and improve transient performance through observer based estimation. This paper is organized as follows. We first outline our prior approach of transient control using the invariant property and demonstrate its applicability for two different SOFC configurations. Next we develop the observer based method for both configurations. Finally we show simulation results and provide concluding remarks.

TRANSIENT CONTROL BASED ON STEADY-STATE INVARIANT PROPERTY

In prior research, we have established the feasibility of transient control through the use of a steady-state property relating fuel utilization U, fuel flow rate $\dot{N}_f$ and fuel cell current draw i_{fc}. The approach is outlined in Fig.1 where OL and CR refer to open-loop and current regulated modes respectively. The later mode of operation leads to transient control of U and the former (i.e. OL) is provided to show the improvement achieved in comparison to unregulated operation. In Fig.1, Eqs.(15) and (16) refer to the steady-state property and the fuel supply system (FSS) represents fuel pumps and/or valves that supply fuel or air-fuel mixture to the reformer. The subscript d is used to represent demanded fuel ($\dot{N}_{f,d}$) or current ($i_{fc,d}$), as opposed to actual fuel ($\dot{N}_f$) or current (i_{fc}). The rest of the figure is self-explanatory.

The method is verified through simulations of two different SOFC system models (systems 1 and 2), shown schematically in Figs.2 and 3. Both are control-oriented models, incorporating heat transfer, thermodynamics, chemical kinetics, electrochemistry and pressure dynamics phenomena in details. Further details about the models in Figs.2 and 3 can be found in [14] and [15] respectively. Both systems use methane as fuel. However, the two primary differences between the systems are:

1. System 1 uses a steam reformer. Pure methane is supplied to the reformer where it is mixed with steam. In contrast, System 2 uses a Partial Oxidation (POX) reformer. Here a mixture of methane and air with a known $O2C$ ratio ($O2C$ ratio is defined as the ratio of molar concentration of molecular oxygen to that of methane in the air-fuel mixture) is supplied to the reformer.
2. The tubular SOFC system uses recirculation for supplying steam to the steam reformer, as shown in Fig.2. Recirculation routes a known fraction k of the steam-rich anode exhaust flow into the steam reformer.

Note that the FSS is not shown in the schematic diagrams and its location is upstream of the gas mixer in Fig.2 and upstream of the POX reformer in Fig.3. For System 1, the steam reforming reactions occurring in the reformer and anode are given by Eqs.(1)-I, II, and III.

$$\begin{array}{llll} \text{(I)} & CH_4 + H_2O \leftrightarrow CO + 3H_2 & \text{(II)} & CO + H_2O \leftrightarrow CO_2 + H_2 \\ \text{(III)} & CH_4 + 2H_2O \leftrightarrow CO_2 + 4H_2 & \text{(IV)} & H_2 + O^{2-} \rightarrow H_2O + 2e \end{array} \tag{1}$$

Denoting r_1, r_2 and r_3 as the rates of reactions I, II, and III, we have $(r_1 + r_3)$, $(-r_1 + r_2)$, $-(r_2 + r_3)$, $-(3r_1 + r_2 + 4r_3)$, $(r_1 + r_2 + 2r_3)$, as the rates of consumption of CH_4, CO, CO_2, H_2 and H_2O respectively. Denoting $\mathcal{R}_{1,r}$, $\mathcal{R}_{2,r}$ and $\mathcal{R}_{1,a}$, $\mathcal{R}_{2,a}$ to represent the rates of formation of CH_4 and CO in the reformer and anode respectively, the mass balance equations for the reformer and anode are

$$\begin{array}{l} \frac{d}{dt}(N_r\mathcal{X}_{1,r}) = k\dot{N}_o\mathcal{X}_{1,a} - \dot{N}_{in}\mathcal{X}_{1,r} + \mathcal{R}_{1,r} + \dot{N}_f \\ \frac{d}{dt}(N_r\mathcal{X}_{2,r}) = k\dot{N}_o\mathcal{X}_{2,a} - \dot{N}_{in}\mathcal{X}_{2,r} + \mathcal{R}_{2,r} \\ \frac{d}{dt}(N_r\mathcal{X}_{3,r}) = k\dot{N}_o\mathcal{X}_{3,a} - \dot{N}_{in}\mathcal{X}_{3,r} - \mathcal{R}_{1,r} - \mathcal{R}_{2,r} \\ \frac{d}{dt}(N_r\mathcal{X}_{4,r}) = k\dot{N}_o\mathcal{X}_{4,a} - \dot{N}_{in}\mathcal{X}_{4,r} - 4\mathcal{R}_{1,r} - \mathcal{R}_{2,r} \\ \frac{d}{dt}(N_r\mathcal{X}_{5,r}) = k\dot{N}_o\mathcal{X}_{5,a} - \dot{N}_{in}\mathcal{X}_{5,r} + 2\mathcal{R}_{1,r} + \mathcal{R}_{2,r} \end{array} \tag{2}$$

$$\begin{array}{l} \frac{d}{dt}(N_a\mathcal{X}_{1,a}) = \dot{N}_{in}\mathcal{X}_{1,r} - \dot{N}_o\mathcal{X}_{1,a} + \mathcal{R}_{1,a} \\ \frac{d}{dt}(N_a\mathcal{X}_{2,a}) = \dot{N}_{in}\mathcal{X}_{2,r} - \dot{N}_o\mathcal{X}_{2,a} + \mathcal{R}_{2,a} \\ \frac{d}{dt}(N_a\mathcal{X}_{3,a}) = \dot{N}_{in}\mathcal{X}_{3,r} - \dot{N}_o\mathcal{X}_{3,a} - \mathcal{R}_{1,a} - \mathcal{R}_{2,a} \\ \frac{d}{dt}(N_a\mathcal{X}_{4,a}) = \dot{N}_{in}\mathcal{X}_{4,r} - \dot{N}_o\mathcal{X}_{4,a} - 4\mathcal{R}_{1,a} - \mathcal{R}_{2,a} - r_e \\ \frac{d}{dt}(N_a\mathcal{X}_{5,a}) = \dot{N}_{in}\mathcal{X}_{5,r} - \dot{N}_o\mathcal{X}_{5,a} + 2\mathcal{R}_{1,a} + \mathcal{R}_{2,a} + r_e \end{array} \tag{3}$$

respectively, where

$$r_e = i_{fc}\mathcal{N}_{cell}/nF \tag{4}$$

is the rate of electro-chemical reaction Eq.(1)-IV. $\dot{N}_o$, $\dot{N}_{in}$ and $\dot{N}_f$ are shown in Fig.2, subscripts 1 through 5 represent the species CH_4, CO, CO_2, H_2 and H_2O in that order, subscripts r and a represent reformer and anode respectively, and N represents molar content. i_{fc} is the fuel cell current, $n = 2$ is the number of electrons participating in an electrochemical reaction and $F = 96485.34$Coul./mole is the Faraday's constant. The aforementioned steady-state property, that forms the basis of this transient control, is derived from the above mass-balance equations. Specifically, noting that U is mathematically defined as follows, [4], [5], [16],

$$U = 1 - \left[\dot{N}_o\left(4\mathcal{X}_{1,a} + \mathcal{X}_{2,a} + \mathcal{X}_{4,a}\right)\right] / \left[\dot{N}_{in}\left(4\mathcal{X}_{1,r} + \mathcal{X}_{2,r} + \mathcal{X}_{4,r}\right)\right] \tag{5}$$

we define two variables ζ_r and ζ_a as follows

$$\begin{array}{l} \zeta_r = 4\mathcal{X}_{1,r} + \mathcal{X}_{2,r} + \mathcal{X}_{4,r} \\ \zeta_a = 4\mathcal{X}_{1,a} + \mathcal{X}_{2,a} + \mathcal{X}_{4,a} \end{array} \quad \Rightarrow \quad U = 1 - \dot{N}_o\zeta_a/\dot{N}_{in}\zeta_r \tag{6}$$

From Eqs.(2), (3), (4) and (6) we have

$$\begin{array}{l} \frac{d}{dt}(N_r\zeta_r) = k\dot{N}_o\zeta_a - \dot{N}_{in}\zeta_r + 4\dot{N}_f \\ \frac{d}{dt}(N_a\zeta_a) = -\dot{N}_o\zeta_a + \dot{N}_{in}\zeta_r + i_{fc}\mathcal{N}_{cell}/nF \end{array} \tag{7}$$

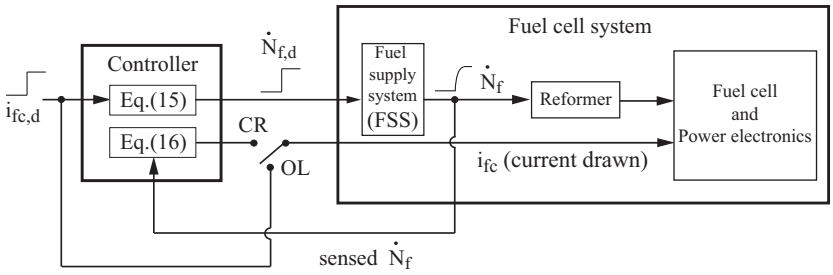

Figure 1. SCHEME FOR TRANSIENT UTILIZATION CONTROL

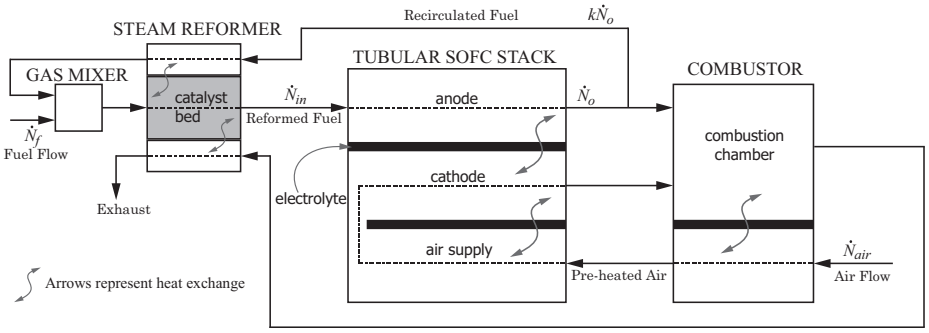

Figure 2. SCHEMATIC DIAGRAM FOR A TUBULAR SOFC WITH STEAM REFORMING - SYSTEM 1

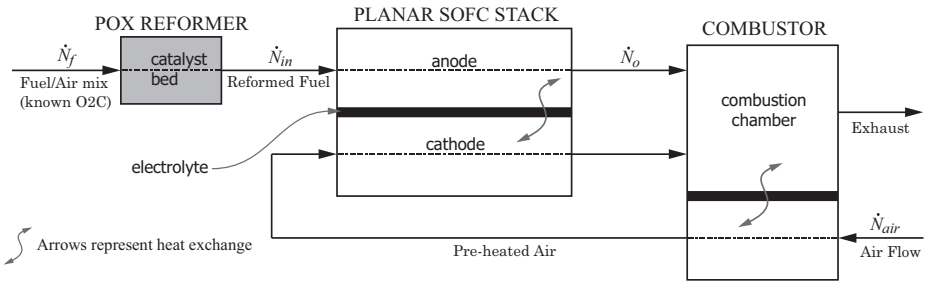

Figure 3. SCHEMATIC DIAGRAM FOR A PLANAR SOFC WITH POX REFORMING - SYSTEM 2

At steady-state, we have from Eq.(7)

$$U_{ss} = (1-k)/\left[\left(4nF\dot{N}_f/i_{fc}\mathcal{N}_{cell}\right)-k\right] \tag{8}$$

Note that Eq.(8) is independent of the unknown rates $\mathcal{R}_{1,r}$, $\mathcal{R}_{2,r}$, $\mathcal{R}_{1,a}$ $\mathcal{R}_{2,a}$, the flow rates $\dot{N}_{in}, \dot{N}_o$, temperatures and pressures. Furthermore, since k, i_{fc} and $\dot{N}_f$ are measurable and known, Eq.(8) is used for open-loop control to achieve a target U_{ss}.

For System 2 in Fig.3, the anode reactions are I through IV of Eq.(1). In the POX reformer, in addition to reactions I, II and III of Eq.(1), the following oxidation reactions occur [17–19]

$$\begin{array}{ll} \text{(V)} & CH_4 + 0.5O_2 \rightarrow CO + 2H_2 \\ \text{(VI)} & CH_4 + 2O_2 \rightarrow CO_2 + 2H_2O \\ \text{(VII)} & CO + 0.5O_2 \rightarrow CO_2 \\ \text{(VIII)} & H_2 + 0.5O_2 \rightarrow H_2O \end{array} \tag{9}$$

with varied and unknown reaction rates. We denote the net rate of oxidation of CH_4 to be R_{ox}, γ to be the fraction of oxidized CH_4 undergoing reaction V, α to be the fraction of H_2 generated by V to be oxidized through VII and β to be the fraction of CO generated by V to be oxidized through VII. Then the net oxidation reaction is

$$\begin{aligned} CH_4 + & [0.5\gamma + 2(1-\gamma) + \gamma\alpha + 0.5\gamma\beta]O_2 \rightarrow \\ & (1-\beta)\gamma CO + 2(1-\alpha)\gamma H_2 + (1-\gamma+\gamma\beta)CO_2 \\ & + 2(1-\gamma+\gamma\alpha)H_2O \end{aligned} \tag{10}$$

The reformer mass balance equations are therefore:

$$\begin{aligned} \tfrac{d}{dt}(N_r\mathcal{X}_{1,r}) &= -\dot{N}_{in}\mathcal{X}_{1,r} + \mathcal{R}_{1,r} - R_{ox} + \dot{N}_f\mathcal{X}_{1,f} \\ \tfrac{d}{dt}(N_r\mathcal{X}_{2,r}) &= -\dot{N}_{in}\mathcal{X}_{2,r} + \mathcal{R}_{2,r} + R_{ox}(1-\beta)\gamma \\ \tfrac{d}{dt}(N_r\mathcal{X}_{3,r}) &= -\dot{N}_{in}\mathcal{X}_{3,r} - \mathcal{R}_{1,r} - \mathcal{R}_{2,r} + R_{ox}(1-\gamma+\gamma\beta) \\ \tfrac{d}{dt}(N_r\mathcal{X}_{4,r}) &= -\dot{N}_{in}\mathcal{X}_{4,r} - 4\mathcal{R}_{1,r} - \mathcal{R}_{2,r} + 2R_{ox}(1-\alpha) \\ \tfrac{d}{dt}(N_r\mathcal{X}_{5,r}) &= -\dot{N}_{in}\mathcal{X}_{5,r} + 2\mathcal{R}_{1,r} + \mathcal{R}_{2,r} + 2R_{ox}(1-\gamma+\gamma\alpha) \\ \tfrac{d}{dt}(N_r\mathcal{X}_{6,r}) &= -\dot{N}_{in}\mathcal{X}_{6,r} + \dot{N}_f\mathcal{X}_{6,f} \\ \tfrac{d}{dt}(N_r\mathcal{X}_{7,r}) &= -\dot{N}_{in}\mathcal{X}_{7,r} - R_{ox}[0.5\gamma + 2(1-\gamma) + \gamma\alpha + 0.5\gamma\beta] \\ & \quad + \dot{N}_f\mathcal{X}_{7,f} \end{aligned} \tag{11}$$

where the subscripts 6 and 7 represent N_2 and O_2 respectively. $\mathcal{X}_{1,f}$, $\mathcal{X}_{6,f}$ and $\mathcal{X}_{7,f}$ represent the known molar fractions of CH_4, N_2 and O_2 respectively in fuel. The relevant anode mass balance equations are same as in Eq.(3). Since oxygen is completely consumed in the POX reformer, we have from Eq.(11),

$$\begin{aligned} R_{ox} &= \dot{N}_f \mathcal{X}_{7,f} / \left[0.5\gamma + 2(1-\gamma) + \gamma\alpha + 0.5\gamma\beta\right] \\ &= \dot{N}_f O2C \mathcal{X}_{1,f} / \left[0.5\gamma + 2(1-\gamma) + \gamma\alpha + 0.5\gamma\beta\right] \end{aligned} \tag{12}$$

where $O2C$ is the oxygen to methane ratio. From Eqs.(3), (4), (6), (11) and (12), we have

$$\begin{aligned} \tfrac{d}{dt}\left(N_r \zeta_r\right) &= -\dot{N}_{in}\zeta_r + 2\dot{N}_f \mathcal{X}_{1,f}(2 - O2C) \\ \tfrac{d}{dt}\left(N_a \zeta_a\right) &= -\dot{N}_o \zeta_a + \dot{N}_{in}\zeta_r + i_{fc}\mathcal{N}_{cell}/nF \end{aligned} \tag{13}$$

Eq.(13) leads to the following steady-state relationship, [15]:

$$U_{ss} = i_{fc}\mathcal{N}_{cell} / \left[2nF\dot{N}_f \mathcal{X}_{1,f}(2 - O2C)\right] \tag{14}$$

Now consider the transient utilization control approach shown in Fig.1, which is applicable for both Systems 1 and 2 in Figs.2 and 3 respectively. Here the demanded fuel cell current is $i_{fc,d}$. Then, from Eqs.(8) and (14), the corresponding fuel demand $\dot{N}_{f,d}$, that satisfies a target U_{ss} is,

$$\dot{N}_{f,d} = \begin{cases} i_{fc,d}\mathcal{N}_{cell}\left[1 - (1 - U_{ss})\,k\right] / 4nFU_{ss} & \text{System 1} \\ i_{fc,d}\mathcal{N}_{cell} / \left[2nF\mathcal{X}_{1,f}U_{ss}(2 - O2C)\right] & \text{System 2} \end{cases} \tag{15}$$

In the OL mode, $i_{fc} = i_{fc,d}$. Hence, in this mode the fuel cell is directly exposed to external power fluctuations. On the other hand, in current regulated (CR) mode, instantaneous i_{fc} is determined using the steady-state property (Eqs.(8) and (14)) and a measurement of the fuel flow $\dot{N}_f$ measured after the fuel supply system but upstream of the reformer, as follows:

$$i_{fc} = \begin{cases} 4nFU_{ss}\dot{N}_f / \mathcal{N}_{cell}\left[1 - (1 - U_{ss})\,k\right] & \text{System 1} \\ 2nFU_{ss}\dot{N}_f \mathcal{X}_{1,f}(2 - O2C) / \mathcal{N}_{cell} & \text{System 2} \end{cases} \tag{16}$$

It must be noted that with this approach, the knowledge of the dynamics of the FSS is not required. The FSS, which consists of a fuel pump and/or valves, will have an in-built controller for fuel flow control. The CR approach outlined in Fig.1, by using the direct measurement of $\dot{N}_f$, bypasses the need to characterize the closed-loop response of the FSS. It is noted that the measurement $\dot{N}_f$ occurs upstream of the reformer where the flow is pure methane or a combination of methane and air.

The improvement in transient response due to CR is demonstrated in the simulations for System 1, shown in Fig.4. In

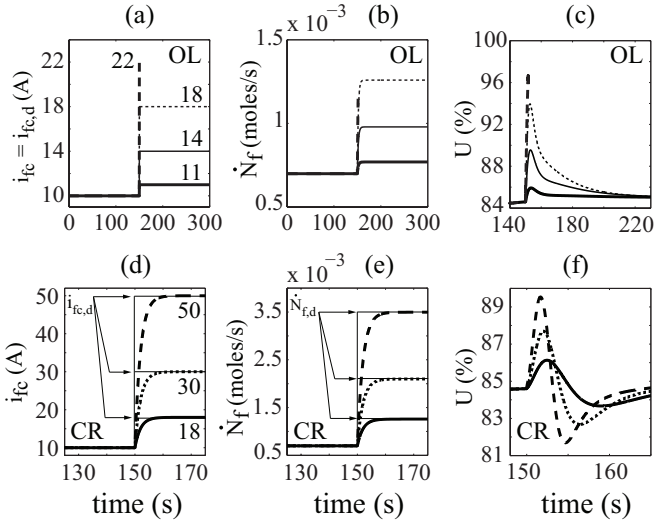

Figure 4. COMPARISON OF OL AND CR MODES - SYSTEM 1

these simulations, the tubular SOFC model, with cell length of 50cm and cell area of 251cm^2, is run with $\mathcal{N}_{cell} = 50$, $\dot{N}_f = 7 \times 10^{-4}$moles/s, $i_{fc} = 10$A for $t < 150$s and various step changes applied on $i_{fc,d}$ for $t > 150$s. These conditions yield a steady state utilization of $U_{ss} \approx 85\%$. Figs.4(a), (b) and (c) show results under OL operation, whereas Figs.4(d), (e) and (f) show results under CR operation. It is evident from the results above that the CR mode drastically reduces transient U. For instance, the step change to $i_{fc,d} = 18$A led to a deviation in U up to $\approx 94\%$ in the open-loop mode Fig.4(c), and only $\approx 86\%$ in CR mode Fig.4(f). Current regulation also increases the transient current handling capability of the fuel cell by a considerable margin. Even with a step change to $i_{fc,d} = 50$A, transient U remains within a $\pm 5\%$ range.

Similar observations made from simulations of system 2, shown in Fig.5. In these simulations, the planar SOFC model, with cell length and width of 10cm each, is run with $\mathcal{N}_{cell} = 30$, $\dot{N}_f = 3 \times 10^{-3}$moles/s, $O2C = 0.5$ and $i_{fc} = 15$A for $t < 100$s. These conditions yield a steady state utilization of $U_{ss} \approx 85\%$. Simulations are shown with step changes on $i_{fc,d}$ to $20, 30$A for $t > 100$s, (Figs.5(a), (d)). As with system 1, the significant fluctuations in U in the OL mode are considerably attenuated in the CR mode, as evident from Figs.5(c) and (f).

DELAYS DUE TO FSS AND REFORMER

It is observed that the transient deviation of U from target U_{ss} is due to the delay introduced along the fuel path. We attribute this delay to two primary factors,

D1: The lag between $\dot{N}_{f,d}$ and $\dot{N}_f$ introduced by dynamics of the FSS, and

D2: The delay introduced by the dynamics of the reformer.

The CR mode of operation compensates for D1. The residual transient in U shown in Fig.4(f) is attributed to D2. For perfect

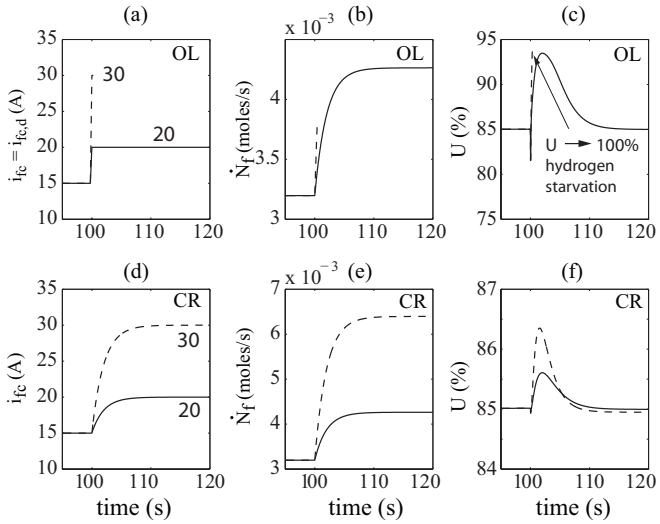

Figure 5. COMPARISON OF OL AND CR MODES - SYSTEM 2

disturbance rejection, i_{fc} must be further regulated, based on the reformer dynamics, to compensate for delay D2. In the following section we will develop an observer based method for compensating for both D1 and D2.

OBSERVER BASED TRANSIENT CONTROL OF U

We note that in the existing method for transient control, the current regulation is based on the measurement $\dot{N}_f$ that occurs upstream of the reformer, shown in Fig.1. Hence while incorporating the delay due to FSS, the delay D2 introduced by the reformer is not incorporated by the current regulation. To incorporate the effect of D2 we first design a nonlinear observers for the two systems under consideration.

System 1

For System 1, based on Eq.(7), we propose the following observer equations:

$$\begin{aligned} N_r\dot{\hat{\zeta}}_r &= k\dot{N}_o\hat{\zeta}_a - \dot{N}_{in}\hat{\zeta}_r + 4\dot{N}_f \\ N_a\dot{\hat{\zeta}}_a &= -\dot{N}_o\hat{\zeta}_a + \dot{N}_{in}\hat{\zeta}_r + i_{fc}\mathcal{N}_{cell}/nF \end{aligned} \tag{17}$$

Note that due to the specific definition of ζ_r and ζ_a their dynamic equations, Eq.(7), and hence the observer equations Eq.(7) are independent of the internal reaction rates. This implies that while observer based species concentration estimation would require concentration sensors [13], estimating ζ_r and ζ_a would not. This is exploited in developing the observer based transient control.

Note that $\dot{N}_f$ is measured, i_{fc} is an input, and $\mathcal{N}_{cell}$, n and F are known constants. In addition, for implementing this observer we assume that the measurements of the bulk flow rates $\dot{N}_{in}$ and $\dot{N}_o$ are available, and the average temperature and pressure of the reformer and the anode are available. In this preliminary study, the effect of measurement errors is not incorporated but will be considered in future work. The equation for the error variables $E_r = \zeta_r - \hat{\zeta}_r$ and $E_a = \zeta_a - \hat{\zeta}_a$ are:

$$\begin{aligned} \dot{\mathbf{E}} &= -A(t)\mathbf{E} + \Delta(t), \\ \mathbf{E} = [E_r\ E_a]^T,\ A(t) &= \begin{bmatrix} \frac{\dot{N}_{in}}{N_r} & -k\frac{\dot{N}_o}{N_r} \\ -\frac{\dot{N}_{in}}{N_a} & \frac{\dot{N}_o}{N_a} \end{bmatrix},\ \Delta = \begin{bmatrix} -\frac{\dot{N}_r\zeta_r}{N_r} & -\frac{\dot{N}_a\zeta_a}{N_a} \end{bmatrix}^T \end{aligned} \tag{18}$$

Considering $\Delta(t)$ to be the input in Eq.(18), the origin of the unforced system $\dot{\mathbf{E}} = -A(t)\mathbf{E}$ is globally exponentially stable since due to finite operating conditions, $A(t)$ and $\dot{A}(t)$ are bounded and the pointwise eigenvalues of $A(t)$ are negative and real, [20]. Hence, the system in Eq.(18) is *Input-to-State-Stable* (ISS), [21]. Therefore $\|\mathbf{E}\|$ is ultimately bounded by a class $\mathcal{K}$ function of $\sup(\|\Delta(t)\|)$. Thus, as $\|\Delta(t)\| \to 0$ so will $\|\mathbf{E}\|$, confirming ultimate-boundedness property of $\|\mathbf{E}\|$. This shows that the proposed observer will provide bounded estimate of ζ_r with the estimation error dependent on the magnitude of $\Delta(t)$. At steady-state $\hat{\zeta}_r$ will provide the correct estimate.

Then from Eqs.(6) and (7), and noting that the measurement of $\dot{N}_{in}$ and the estimate $\hat{\zeta}_r$ are available, the current regulation (CR) method can be modified from that given in Fig.1 and Eq.(16) to the following:

$$U_{ss} = i_{fc}\mathcal{N}_{cell}/nF\dot{N}_{in}\zeta_r \quad \Rightarrow \quad i_{fc} = U_{ss}nF\dot{N}_{in}\hat{\zeta}_r/\mathcal{N}_{cell} \tag{19}$$

System 2

For System 2, based on Eq.(13) we have the following observer equation:

$$N_r\dot{\hat{\zeta}}_r = -\dot{N}_{in}\hat{\zeta}_r + 2\dot{N}_f(2 - O2C) \tag{20}$$

As with System 1, we can show that the error $E_r = \zeta_r - \hat{\zeta}_r$ will be bounded and will depend on the magnitude of $\Delta(t) = -\dot{N}_r\zeta_r/N_r$. For this system the regulated fuel cell current i_{fc} using the observer based method will be same as in Eq.(19). The observer based approach is outlined in Fig.6. We make the following general observations about the proposed observer based method:

1. CR in the observer-based approach uses $\dot{N}_{in}\hat{\zeta}_r$, which is an estimate of available hydrogen downstream of the reformer and at the inlet to the anode. Therefore, this approach is expected to compensate for the delay D2, at least partially.
2. The analytical development of the observer relies on the independence of ζ_r and ζ_a on internal reaction rates. This holds for both systems 1 and 2.
3. The observers do not allow controlling the rate of error-convergence. From Eqs.(17), (18) and (20), it is evident that the rate of convergence will be higher for smaller (reformer and/or anode) volumes and larger flow rates.

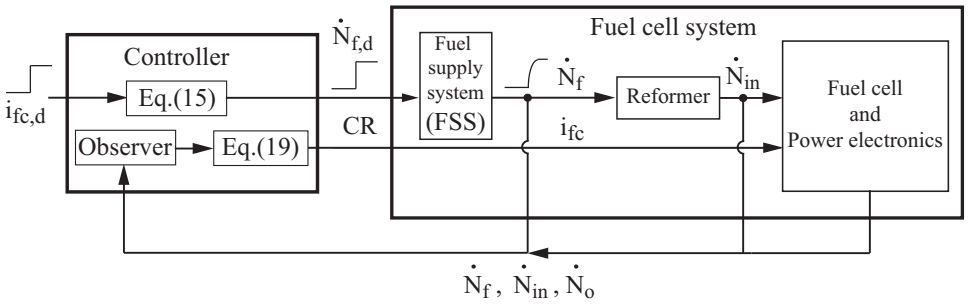

Figure 6. OBSERVER-BASED APPROACH FOR TRANSIENT UTILIZATION CONTROL

SIMULATION RESULTS

System 1

The SOFC system simulated is same as in Fig.4 with target $U_{ss} = 85\%$, $i_{fc,d} = 10$A for $t < 150$s, and $20, 30, 50$A for $t \geq 150$s. For each step change in $i_{fc,d}$, we compare the two approaches outlined in Fig.1 and Fig.6. The simulation results are provided in Fig.7. Note that Figs.7(a), (d) and (g) correspond to step change to 20A, plots (b), (e) and (h) correspond to step change to 30A and plots (c), (f) and (i) correspond to step change to 50A.

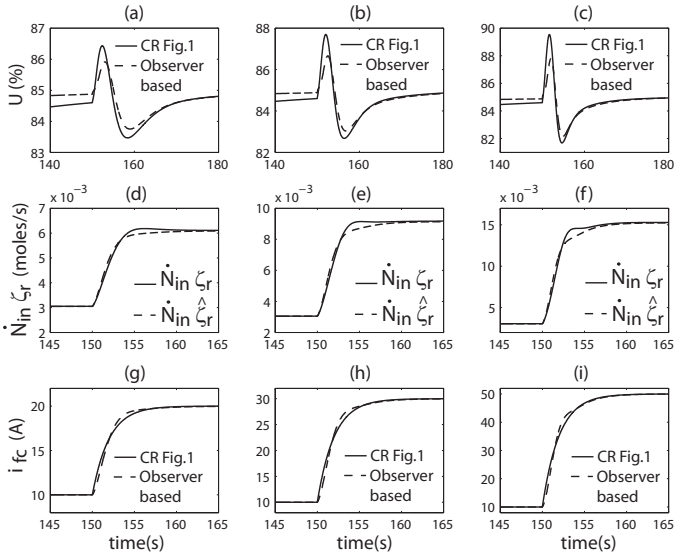

Figure 7. SIMULATION RESULTS FOR OBSERVER-BASED APPROACH FOR TRANSIENT UTILIZATION CONTROL - SYSTEM 1

In Figs.7(a), (b) and (c) we compare the transient utilization obtained by the two methods. Note that the observer based method provides better transient attenuation and its effectiveness is more pronounced for larger power fluctuations. The $\hat{\zeta}$ estimation by the observer is depicted for the three step changes in plots (d), (e) and (f). The transient discrepancies are attributed to $\Delta(t)$, given in Eq.(18). Current regulation through the observer based approach is compared to the existing approach in plots (g), (h) and (i). It is evident from Fig.7 that the observer based approach provides better transient utilization control over the existing approach for System 1.

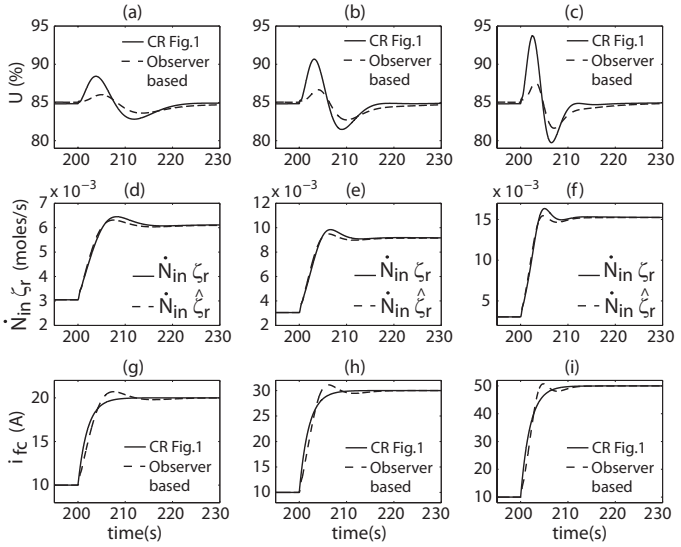

Figure 8. SIMULATION RESULTS FOR OBSERVER-BASED APPROACH FOR TRANSIENT UTILIZATION CONTROL - SYSTEM 1

We next observe that if the delay D2, which is due to the reformer dynamics, is significantly higher than delay D1 induced by the FSS, then the observer based approach may provide a greater benefit. To test this, we artificially increased the reformer volume in System 1 considered above by a factor of 4. Increasing the reformer volume could lead to a slower reformer dynamics if the operating conditions are similar as before, and thereby increase D2. In the above simulation, the volume of the steam-reformer is $6 \times 10^{-4}\text{m}^3$. We increase the steam reformer volume to $2.4 \times 10^{-3}\text{m}^3$ and rerun the simulations shown in Fig.7. The simulation results with increased reformer volume are given in Fig.8. As in the previous simulation, Figs.8(a), (d) and (g) correspond to step change in $i_{fc,d}$ from 10A to 20A, plots (b), (e) and (h) correspond to step change to 30A and plots (c), (f) and (i) correspond to step change to 50A. As expected, the observer-based current regulation approach provides significantly higher transient attenuation in comparison to the existing current regulation approach, as evident from Figs.8(a), (b) and (c).

System 2

The SOFC system simulated is same as in Fig.5 with target $U_{ss} = 85\%$, $i_{fc,d} = 15$A for $t < 100$s, and $20, 30$A for $t \geq 100$s. For each step change in $i_{fc,d}$, we compare the two current regulation approaches outlined in Fig.1 and Fig.6. The simulation results are provided in Fig.9. Note that Figs.9(a), (c) and (e) correspond to step change to 20A, and plots (b), (d) and (f) correspond to step change to 30A.

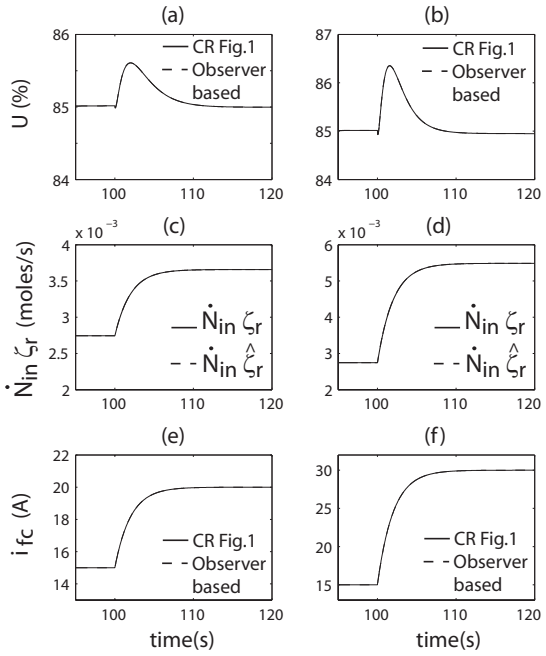

Figure 9. SIMULATION RESULTS FOR OBSERVER-BASED APPROACH FOR TRANSIENT UTILIZATION CONTROL - SYSTEM 2

It is clear from Fig.9 that for system 2, the observer based approach does not provide any noticeable benefit. This is attributed to the fact that in comparison to steam reformers, POX reformers are more compact and have faster response. Hence, the delay D2 is expected to be lower for POX reformers. Unlike System 1, the observer based approach did not yield significant benefit as a result of increasing the volume of the POX reformer in System 2. However, further research needs to be performed for better assessment of the effectiveness of this approach for POX reformer based SOFC systems.

CONCLUSION

In this paper we develop an observer-based method for transient control of SOFCs. The observer estimates an effective available hydrogen at the anode inlet. It uses total flow measurement rather than using sensors for individual species. The fuel cell current is regulated by combining the observed state with a steady-state relation. This approach provides improved transient control of U over an invariant property based method, previously developed by the authors, [12]. In comparison to the original current regulation approach, the observer has increased sensing requirement but does not require a knowledge of the internal reaction rates. The proposed approach is shown to be feasible for two different SOFC systems; however it is found to be more effective for slower reformers. This paper gives a basic design of the observer. Improvements will be attempted and performance of the observer under sensing errors will be investigated in future research.

ACKNOWLEDGMENT

The authors gratefully acknowledge the support provided by the Office of Naval Research under grant #N000140910272 in conducting this research.

REFERENCES

[1] Larminie, J., and Dicks, A., 2003. *Fuel Cell Systems Explained*, second ed. John Wiley & Sons, Inc.

[2] Meacham, J. R., Jabbari, F., Brouwer, J., Mauzey, J. L., and Samuelsen, G. S., 2006. "Analysis of stationary fuel cell dynamic ramping capabilities and ultra capacitor energy storage using high resolution demand data". *Journal of Power Sources,* **156**, pp. 472–479.

[3] Vahidi, A., Stefanopoulou, A., and Peng, H., 2006. "Current management in a hybrid fuel cell power system: A model-predictive control approach". *IEEE Transactions on Control Systems Technology,* **14**(6), pp. 1047 – 1057.

[4] Mueller, F., Brouwer, J., Jabbari, F., and Samuelsen, S., 2006. "Dynamic simulation of an integrated solid oxide fuel cell system including current-based fuel flow control". *ASME Journal of Fuel Cell Science and Technology,* **3**, pp. 144–154.

[5] Lazzaretto, A., Toffolo, A., and Zanon, F., 2004. "Parameter setting for a tubular SOFC simulation model". *ASME Journal of Energy Resources Technology,* **126**, pp. 40–46.

[6] Sedghisigarchi, K., and Feliachi, A., 2002. "Control of grid-connected fuel cell power plant for transient stability enhancement". *Proceedings of the IEEE Power Engineering Society Transmission and Distribution Conference,* **1**, pp. 383–388.

[7] Gaynor, R., Mueller, F., Jabbari, F., and Brouwer, J., 2008. "On control concepts to prevent fuel starvation in solid oxide fuel cells". *Journal of Power Sources,* **180**, p. 330342.

[8] Mueller, F., Jabbari, F., and Brouwer, J., 2009. "On the intrinsic transient capability and limitations of solid oxide fuel cell systems". *Journal of Power Sources,* **187**, pp. 452–460.

[9] Sun, J., and Kolmanovsky, I., 2005. "Load governor for fuel cell oxygen starvation protection: A robust nonlinear reference governor approach". *IEEE Transactions on Control Systems Technology,* **13**(6), pp. 911–920.

[10] Vahidi, A., Kolmanovsky, I., and Stefanopoulou, A., 2007. "Constraint handling in fuel cell system: A fast reference

governor approach". *IEEE Transactions on Control Systems Technology,* **15**(1), pp. 86–98.

[11] Vahidi, A., and Greenwell, W., 2007. "A decentralized model predictive control approach to power management of a fuel cell-ultracapacitor hybrid". *Proceedings of the 2007 American Control Conference*, pp. 5431–5437.

[12] Das, T., and Weisman, R., 2009. "A feedback based load shaping strategy for fuel utilization control in SOFC systems". *American Control Conference, St. Louis, MO.*

[13] Das, T., 2009. "An adaptive observer design for recirculation based solid oxide fuel cell systems using cell voltage measurement". *American Control Conference, St. Louis, MO.*

[14] Das, T., Narayanan, S., and Mukherjee, R., 2010. "Steady-state and transient analysis of a steam reformer based solid oxide fuel cell system". *ASME Journal of Fuel Cell Science and Technology,* **7**(1).

[15] Slippey, A., 2009. "Dynamic modeling and analysis of multiple SOFC system configurations". Master's thesis, Rochester Institute of Technology.

[16] Campanari, S., 2001. "Thermodynamic model and parametric analysis of a tubular SOFC module". *Journal of Power Sources,* **92**, pp. 26–34.

[17] Pukrushpan, J. T., Stefanopoulou, A. G., and Peng, H., 2004. *Control of Fuel Cell Power Systems*. Springer.

[18] Zhu, J., Zhang, D., and King, K. D., 2001. "Reforming of CH_4 by partial oxidation: Thermodynamic and kinetic analyses". *Fuel,* **80**(7), p. 899905.

[19] Horn, R., Williams, K. A., Degenstein, N. J., and Schmidt, L. D., 2007. "Mechanism of H_2 and CO formation in the catalytic partial oxidation of CH_4 on Rh probed by steady-state spatial profiles and spatially resolved transients". *Chemical Engineering Science,* **62**(5), p. 12981307.

[20] Rugh, W. J., 1996. *Linear System Theory*, 2 ed. Prentice Hall, Upper Saddle River, NJ.

[21] Khalil, H., 2002. *Nonlinear Systems*, 3 ed. Prentice-Hall, Inc. Upper Saddle River, NJ.